https://doi.org/10.20965/jaciii.2012.p0841

Paper:

A Mutual-Information-Based Global Matching Method for Chest-Radiography Temporal Subtraction

Qian Yu[*1], **Lifeng He**[*2,*3], **Tsuyoshi Nakamura**[*1], **Yuyan Chao**[*4], **and Kenji Suzuki**[*5]

[*1]Department of Computer Science and Engineering, Nagoya Institute of Technology
Gokiso-cho, Showa-ku, Nagoya, Aichi 466-8555, Japan
E-mail: kasunyu@gmail.com, tnaka@nitech.ac.jp
[*2]College of Electrical & Information Engineering, Shaanxi University of Science and Technology, China
[*3]Graduate School of Information Science and Technology, Aichi Prefectural University, Japan
E-mail: helifeng@ist.aichi-pu.ac.jp
[*4]Graduate School of Environmental Management, Nagoya Sangyo University, Japan
E-mail: chao@nagoya-su.ac.jp
[*5]Department of Radiology, Division of the Biological Sciences, The University of Chicago, USA
E-mail: suzuki@uchicago.edu
[Received April 6, 2012; accepted October 10, 2012]

Lung cancer is the most common cancer in the world. Early detection is most important for reducing death due to lung cancer. Chest radiography has been widely and frequently used for the detection and diagnosis of lung cancer. To assess pathological changes in chest radiographs, radiologists often compare the previous chest radiograph and the current one from the same patient at different times. A temporal subtraction image, which is constructed from the previous and current radiographs, is often used to support this comparison work. This paper presents a Mutual-Information (MI)-based global matching method for chest-radiography temporal subtraction. We first make a preliminary transformation on the previous radiograph to make the center line of the lungs in the previous radiograph coincide with that of the current one. Then, we specify areas of the lungs to be used for mutual information registration and extract rib edges in these areas. We transform the rib edge image of the previous radiograph until mutual information between the rib edge image of the previous radiograph and that of the current radiograph becomes maximal. Finally, we use the same transform parameters to transform the previous radiograph, and then use the current radiograph and the transformed previous radiograph to construct the temporal subtraction image. The experimental result demonstrates that our proposed method can enhance pathological changes and reduces misregistration artifacts.

Keywords: temporal subtraction, mutual information (MI), chest radiography, image registration, computer aided diagnosis (CAD)

1. Introduction

Lung cancer has been the most common cancer in the world for several decades and by 2008, there were an estimated 1.61 million new cases, representing 12.7% of all new cancers. The majority of cases now occur in developing countries (55%). Lung cancer is still the most common cancer among men worldwide (1.1 million cases, 16.5% of the total). In females, incidence rates are generally lower, but worldwide, lung cancer is now the fourth most frequent cancer among women (513000 cases, 8.5% of all cancers) and the second most common cause of death from cancer (427000 deaths, 12.8% of the total). Because of its high fatality rate (the ratio of mortality to incidence is 0.86) and the lack of variability in survival in developed and developing countries, the highest and lowest mortality rates are estimated in the same regions among both in men and women [1].

Early detection is most important for reducing death due to lung cancer. Chest radiography has been widely and frequently used for the detection and diagnosis of lung cancer. To assess pathological changes in chest radiographs, radiologists often compare the previous and current chest radiographs obtained from the same patient at different times. To support this comparison work, a temporal subtraction image, which is constructed from previous and current radiographs, is often used. The temporal subtraction image enhances pathological changes, reduces the visual load on radiologists, prevents overlooks and increases diagnostic accuracy.

Because previous and current radiographs are taken at different times, photographic conditions such as the patient's posture, X-ray conditions, state of radio devices and so on are usually different. This makes accurate image registration a challenge process. Because artifacts due to misregistration may lead to misdiagnosis, registration accuracy is crucial. Ishida et al. proposed an image registration method for this purpose, that first makes global

matching [2] in the lung area, then makes local matching [3] to correct misregistration in local chest area in detail. Armato et al. used automatic evaluation to develop registration accuracy [4]. Inaba et al. proposed another registration method [5] but the quality of global matching was not enough.

This paper presents a Mutual-Information (MI)-based global matching method for chest-radiography temporal subtraction. We first make preliminary transformation on the previous radiograph to make the center line of the lungs in the previous radiograph coincide with that of the current radiograph. Then, we specify areas of the lungs to be used for mutual information registration and extract rib edges in these areas. We transform the rib edge image of the previous radiograph until mutual information [6] between the rib edge image of the previous radiograph and that of the current radiograph becomes maximal. Finally, we use the same transform parameters to transform the previous radiograph, and then use the current radiograph and the transformed previous radiograph to construct the temporal subtraction image.

This paper is organized as follows: Section 2 introduces mutual information in image registration. We describe our proposed global matching method for chest-radiograph temporal subtraction in detailed in Section 3. We then show and discuss results in Section 4, and present our conclusion in Section 5.

2. Mutual Information in Image Registration

Two discrete random variables X and Y with marginal probability distributions $p_X(x)$ and $p_Y(y)$, where x, y are the values that X and Y may take, and joint probability distribution $p_{XY}(x,y)$ are statistically independent if $p_{XY}(x,y) = p_X(x)p_Y(y)$, while they are maximal dependent if they are relational. Mutual information $I(X,Y)$ of X and Y measures the degree of dependence of X and Y as the distance between joint distribution $p_{XY}(x,y)$ and distribution associated with the case of complete independence $p_X(x)p_Y(y)$ [7], i.e.,

$$I(X,Y) = \sum_{x,y} p_{XY}(x,y) \log \frac{p_{XY}(x,y)}{p_X(x)p_Y(y)}. \quad \ldots (1)$$

Mutual Information (MI) is related to the information theoretic notion of entropy by the following equations:

$$I(X,Y) = H(X) + H(Y) - H(X,Y) \quad \ldots (2)$$

where $H(X)$ and $H(Y)$ are the entropy of X and that of Y respectively, and $H(X,Y)$ the joint entropy of X and Y. Essentially, entropy is a measure of uncertainty – the higher the entropy of a random variable, the more uncertain it is.

For gray level image A with N pixels, entropy is used to measure the uncertainty of pixels in the image, which is defined as

$$H(A) = -\sum_{i=0}^{N-1} p(a_i) \log p(a_i) \quad \ldots (3)$$

where $p(a_i)$ means the probability of gray level a_i in image A, and it can be obtained from the image histogram as follows:

$$p(a_i) = \frac{h(a_i)}{N} \quad \ldots (4)$$

where $h(a_i)$ is the histogram value of a_i in the image.

The joint entropy of two images A and B with N pixels, namely $H(A,B)$, is defined as

$$H(A,B) = -\sum_{i=0}^{N-1} \sum_{j=0}^{N-1} p(a_i,b_j) \log p(a_i,b_j) \quad \ldots (5)$$

where $p(a_i,b_j)$ means the joint probability of gray level a_i in image A and gray level b_i in image B, which is obtained as

$$p(a_i,b_j) = \frac{h(a_i,b_j)}{N} \quad \ldots (6)$$

where $h(a_i,b_j)$ is the 2-D histogram value. It denotes the account of pixels for which, at the same coordinate, the gray level in image A is a_i and the gray level in image B is b_j.

Last, mutual information of the two images A and B is defined as

$$I(A,B) = \frac{1}{N} \sum_{i=0}^{N-1} \sum_{j=0}^{N-1} h(a_i,b_j) \log \frac{Nh(a_i,b_j)}{h(a_i)h(b_j)} p(a_i,b_j). \quad \ldots (7)$$

In a chest-radiograph registration problem, although the previous and current radiographs are taken at different times, their information comes from the same human anatomy construction. Thus, in image registration, when the same spatial information of the two images is greatest, the mutual information of their corresponding pixels is also maximal.

Mutual-information-based image registration for images A and B is to find an optimum transformation $T(B)$ of B such that the mutual information of image A and $T(B)$ is maximal.

3. Mutual-Information-Based Global Matching

Figure 1 shows an example of the original previous radiograph (**Fig. 1(a)**) and current radiograph (**Fig. 1(b)**) of a patient, namely Case 1. The original radiographs use 16-bit raw image format. We use this example to introduce our matching process in this section.

3.1. Preliminary Transformation

The purpose for constructing a temporal subtraction image is to enhance pathological changes in lungs and weaken normal tissue. Thus, we only need to consider lung regions of radiographs. Therefore, we should first extract lung regions of radiographs.

The gray values of the original radiograph can be di-

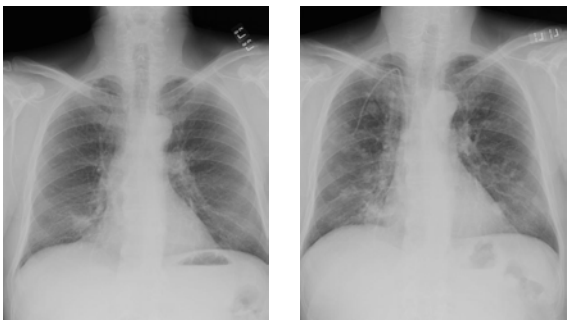

(a) Previous (b) Current

Fig. 1. Original radiographs used in temporal subtraction.

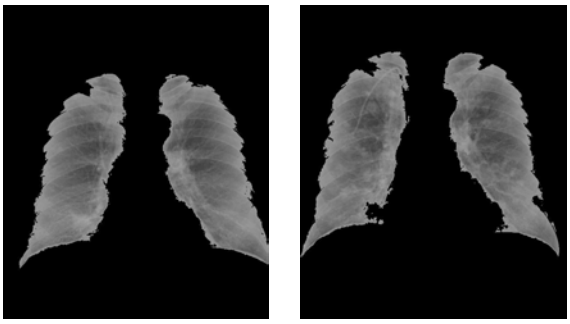

(a) Previous (b) Current

Fig. 2. Extracted images of lung regions.

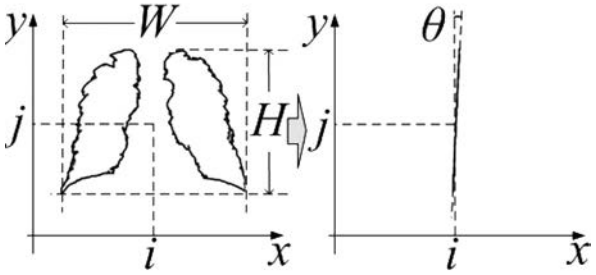

Fig. 3. Spatial data of lung regions.

vided into three parts: a background region with low gray levels, a lung region with medium gray levels, and a skeletal region with high gray levels. According to these features, we extract lung regions from radiographs by multivalue processing. The images of lung regions extracted from the previous and current radiographs in Case 1 are shown in **Figs. 2(a)** and **(b)**, respectively.

Next, similar to the previous method proposed in Ref. [2], we extract the outer contours of lungs for each extracted image of lung regions and derive midpoints of lungs. Then, by linear fitting on these points, we get the center line of the lungs. Moreover, we can obtain the spatial data for the lungs from the image of lung regions, such as the average lung width (W), the average lung height (H), and the center point coordinate (i, j) of the lungs, as shown in **Fig. 3**.

Comparing the above data of the previous and current images, we get preliminary transformation parameters $\omega_0 = \{r_{x_0}, r_{y_0}, d_{x_0}, d_{y_0}, \theta_0\}$, where r_{x_0} and r_{y_0} are ratios of width and length between lung regions of previous

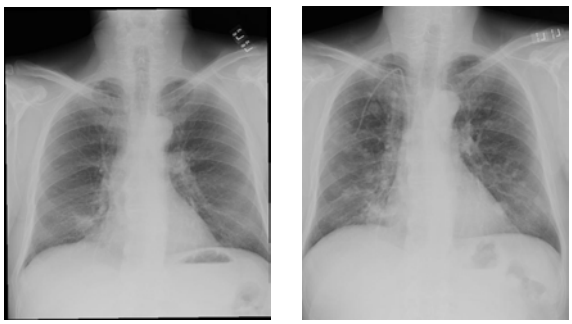

(a) Previous (b) Current

Fig. 4. Radiographs after preliminary transformation.

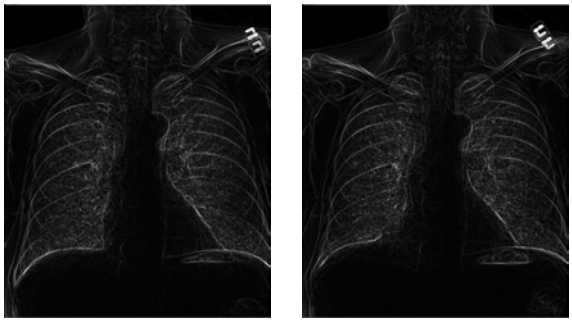

(a) Previous (b) Current

Fig. 5. Sobel edge images.

and current radiographs, d_{x_0} and d_{y_0} are the horizontal distance and vertical distance of the two center points, and θ_0 is the angle of the two center lines. We rotate the previous radiograph according to the angle, and then shift it to make its centerline coincide with that of the current radiograph. Images after preliminary transformation are shown in **Fig. 4**.

3.2. Determining the Areas Used for MI Registration

Respiratory movement makes the shape of lungs in radiographs ever changing. The width and length of the lung in a radiograph are different at different times. Note that the rib cage moves in accordance with respiratory movement. In other words, rib cage status reflects shape changes of the lungs. Because the edges of ribs in lung areas of radiographs represent the state of ribs, we use Sobel edge detection [8] to extract them first, as shown in **Fig. 5**.

If we used all Sobel edges of images for MI registration, the MI of skeleton edges would occupy a large proportion. Skeleton edges, especially the collarbone, may lead to misregistration for lung parenchyma. We need to determine areas that involve the most lung tissues. Using such areas for matching, we can make lung tissues match better and reduce the amount of calculation.

We observed that the edges of lung tissues have middling intensity gradients and that the edges of ribs have large intensity gradients. As shown in **Fig. 6**, by applying Canny edge detection with different thresholds [9] on the previous radiograph, we obtain images that involve rib edges and different amounts of parenchyma

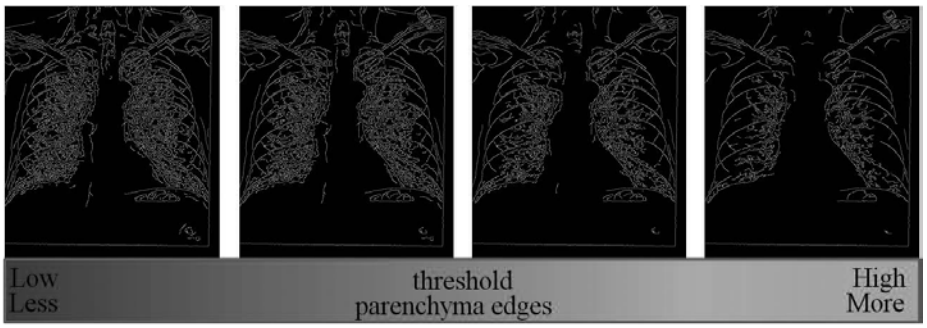

Fig. 6. Canny edge images with different thresholds.

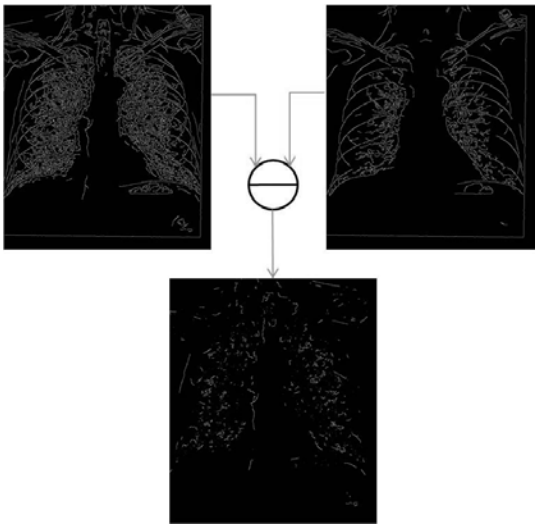

Fig. 7. Subtraction of Canny edge images.

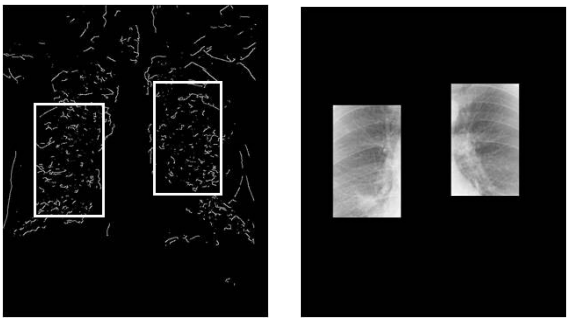

(a) Canny edges (b) Previous radiograph

Fig. 8. The mutual information areas.

edges, respectively. Subtracting the image with few lung parenchyma edges and the image with many lung parenchyma edges, we obtain images that just involve lung parenchyma edges, as shown in **Fig. 7**.

We define areas used for MI registration as two rectangles for left and right lung regions, respectively, each of which has width M and height N.

We change the position of rectangles on derived parenchyma edge images and calculate the amount of parenchyma edges involved at every position in rectangles by use of the labeling algorithm proposed in Ref. [10]. We set the rectangle position such that the amount of parenchyma edges involved in the rectangles is maximal (**Fig. 8**).

For different radiographs, the size of lung regions would be different. If the height of lung regions is H and width is W, we use $R(\alpha,\beta)$ to denote the determined MI areas, where $M=\alpha\times W$, $N=\beta\times H$ and $0\leq\alpha,\beta\leq 1$.

For MI registration, a larger MI area might involve more lung tissue information, but might also involve more other unnecessary information that may reduce registration accuracy. On the other hand, a small MI area may lose much important information. Through experiments on our cases, we find that taking $\alpha=1/3,\beta=3/4$ obtain good matching.

3.3. Obtaining Optimum Transformation

Using preliminary transformation parameter set $\omega_0=\{r_{x_0},r_{y_0},d_{x_0},d_{y_0},\theta_0\}$ derived above as the initial parameter set, we adjust transformation parameters based on mutual information, as shown in **Fig. 9**, where S_p denotes the Sobel edge image in MI areas of the previous radiograph, S_c denotes that of the current radiograph, and $I(A,B)$ is mutual information given in Eq. (7). We transform S_p by adjusting parameters in a certain range of D_ω (**Fig. 10**). A smaller range may lose optimum parameters, but a larger range would take much time for processing. For our cases, we define $r_{x_-}=r_{x_0}-0.1$, $r_{x_+}=r_{x_0}-0.1$, $r_{y_-}=r_{y_0}-0.1$, $r_{y_+}=r_{y_0}+0.1$, $d_{x_-}=d_{x_0}-0.15W$, $d_{x_+}=d_{x_0}+0.15W$, $d_{y_-}=d_{y_0}-0.15H$, $d_{y_+}=d_{y_0}+0.15H$, $\theta_-=\theta_0-15^\circ$, $\theta_+=\theta_0+15^\circ$. Moreover, we take 20 values for each parameter in its scope with the same step value. After each transformation, we compute mutual information between S_c and transformed S_p. If the MI derived by use of these parameters increases, we update parameters. Thus, after we try all parameter sets in our range, we obtain optimum transformation parameters. Then, we transform the previous radiograph by use of the optimum transformation parameters. **Fig. 11** shows the transformed previous image.

In this way, we construct a temporal subtraction image by subtracting the original current radiograph and the transformed previous radiograph.

$I_{max} = 0;$

$\omega_{max} = \omega_0 = \{ r_{x_0}, r_{y_0}, d_{x_0}, d_{y_0}, \theta_0 \};$

$T_{max} = T_0;$

$$D_\omega = \left\{ (r_x, r_y, d_x, d_y, \theta) \middle| \begin{array}{c} r_x \in [r_{x_-}, r_{x_+}], \\ r_y \in [r_{y_-}, r_{y_+}], \\ d_x \in [d_{x_-}, d_{x_+}], \\ d_y \in [d_{y_-}, d_{y_+}], \\ \theta \in [\theta_-, \theta_+] \end{array} \right\};$$

for $\omega = \{ r_x, r_y, d_x, d_y, \theta \} \subseteq D_\omega$ **do**

  $A = T_\omega(S_p);$

  $B = S_c;$

  if $I(A,B) > I_{max}$ **then**

    $\omega_{max} = \omega;$

    $T_{max} = T_\omega;$

  end if

end for

Fig. 9. Parameters adjustment process.

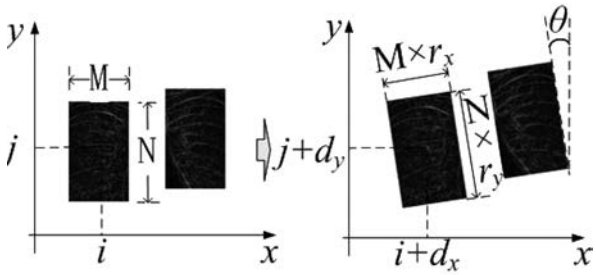

Fig. 10. The transformation of S_p.

Fig. 11. The previous radiograph after transformation.

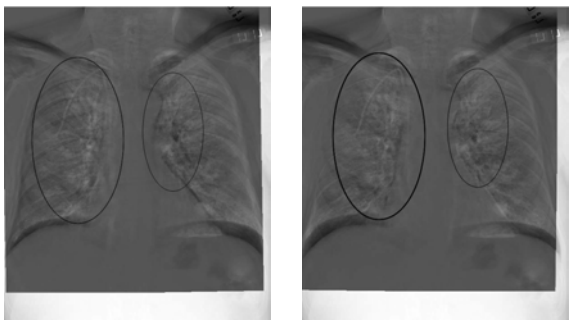

(a) Previous method (b) Proposed method

Fig. 12. Temporal subtraction images of Case 1.

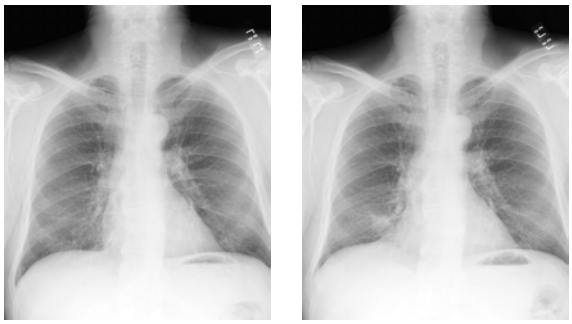

(a) Previous (b) Current

Fig. 13. Original radiographs of Case 2.

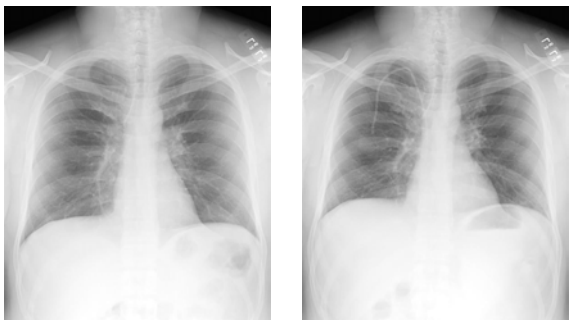

(a) Previous (b) Current

Fig. 14. Original radiographs of Case 3.

4. Experimental Results and Evaluation

A pathological change appears as bright in radiographs. If there is a pathological change in the current radiograph but not in the previous radiograph in the same area, this area will appear bright in the constructed temporal subtraction image. A bright area in the constructed temporal subtraction image unrelated to pathological change is a misregistration artifact, as is a very dark area in the constructed temporal subtraction image.

We use two methods to evaluate the quality of a temporal subtraction image: we evaluate the image by observing whether pathological changes are enhanced and how many misregistration artifacts are there in the subtraction image. **Fig. 12** shows temporal subtraction images constructed by the previous method and our proposed method applied on Case 1, respectively. **Figs. 13** and **14** show other two cases, namely Case 2 and Case 3, respectively.

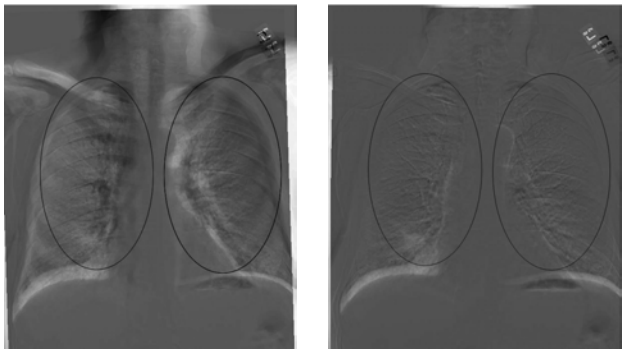

(a) Previous method (b) Proposed method

Fig. 15. Temporal subtraction images of Case 2.

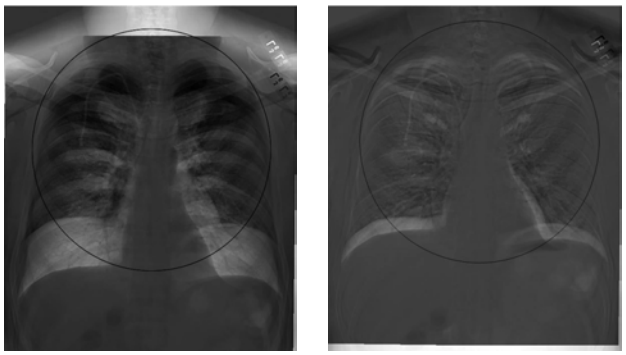

(a) Previous method (b) Proposed method

Fig. 16. Temporal subtraction images of Case 3.

The temporal subtraction images of these two cases constructed by the previous method and that by our proposed method are shown in **Figs. 15** and **16** respectively. Comparing the temporal subtraction images generated by the previous method and the proposed method in these three cases, we can find that there are significant improvements in the visualization of pathological changes in the image constructed by our proposed method. Especially in Case 3, the temporal subtraction image generated by the previous method is unavailable, but that by our proposed method is quite successful. In the other two cases, we can also find that our proposed method matched better and suppressed ribs better in some areas of the image, which can reduce the rib's influence on diagnosis. Moreover, in any case, the temporal subtraction images constructed by our proposed method have fewer misregistration artifacts.

We also use the histogram of pixel values in lung regions to evaluate a temporal subtraction image. Because misregistration areas contain many very dark or very bright pixels, a subtraction image generated by accurate registration usually has low contrast. Therefore, the width of a histogram from a high-quality subtraction image is usually narrow and that of a low-quality one is wide. Similarly, for quantitative comparison of temporal subtraction images, we compare the standard deviation of the pixel value in images. The smaller standard deviation of a temporal subtraction image means the higher quality of the image.

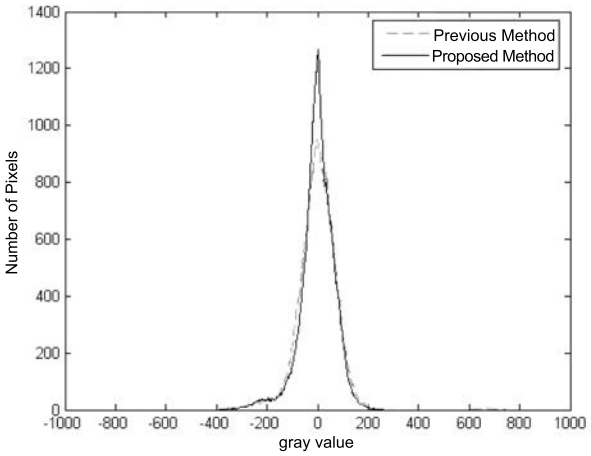

Fig. 17. Lung regions histogram of Case 1.

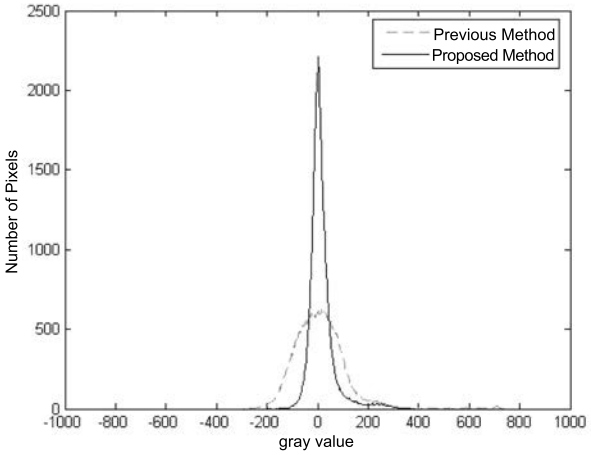

Fig. 18. Lung regions histogram of Case 2.

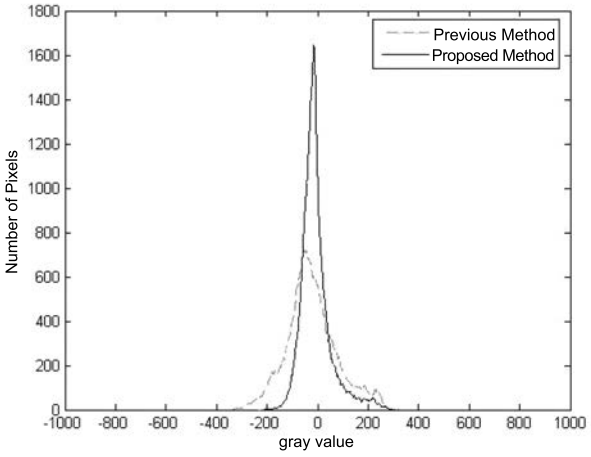

Fig. 19. Lung regions histogram of Case 3.

Because our purpose is to match lung regions only, we simply calculate histograms of lung regions. **Figs. 17**, **18** and **19** show the lung-region histograms of our three cases, respectively. We can find that for each case, the image constructed by the proposed method has a higher peak and narrower width, i.e., the quality of the subtraction im-

Table 1. Standard deviation (σ) and improvement rates.

Case No.	Previous	Proposed	Improvement rate
1	41.068	38.099	7.23%
2	49.670	27.686	44.28%
3	55.157	33.937	38.48%
4	44.544	35.024	21.37%
5	44.944	38.974	13.28%
6	45.760	43.578	4.77%
7	49.970	45.618	8.71%

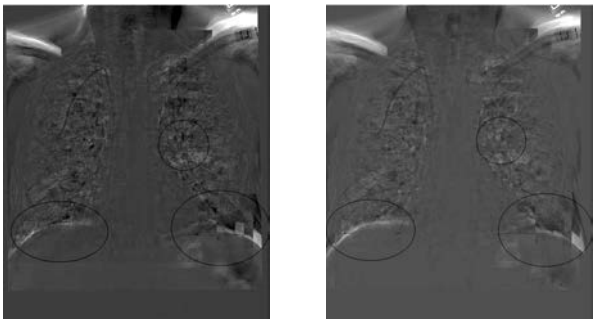

(a) Based on previous global matching (b) Based on proposed global matching

Fig. 20. Temporal subtraction images after local matching of Case 1.

age constructed using our proposed method is better than that by the previous method. **Table 1** shows the standard deviations (σ) and improvement rates of the above three cases and four additional cases.

We improved the global matching method for temporal subtraction. However, there are still some misregistration artifacts occurring in lung regions of constructed temporal subtraction images, which are primarily caused by the physiological activity of the lungs. To reduce such misregistration, we need to do local matching after global matching. For comparison, by using of the previous local matching method proposed in [5], we made local matching on the constructed previous images generated by the previous and our proposed methods in Case 1 respectively. Results are shown in **Fig. 20**. Note that our proposed global method makes some improvement.

We use fuzzy inference for aiding radiologist diagnosis further. The cancerous area appearing as bright in the temporal subtraction image is usually circular. Therefore, we first extract bright areas from the derived temporal subtraction image and calculate the size and circularity of each bright area. Then we use fuzzy c-means algorithm to divide these areas into clusters based on size and circularity data, and compute the fuzzy cluster center of each cluster. Last, based on fuzzy cluster center data, we use the fuzzy inference method to obtain the probability of cancer in areas of each cluster.

In the inference process, we use the trapezoidal function to be membership functions of fuzzy sets. Eq. (8) denotes the membership function $f_A(x)$ of fuzzy set A:

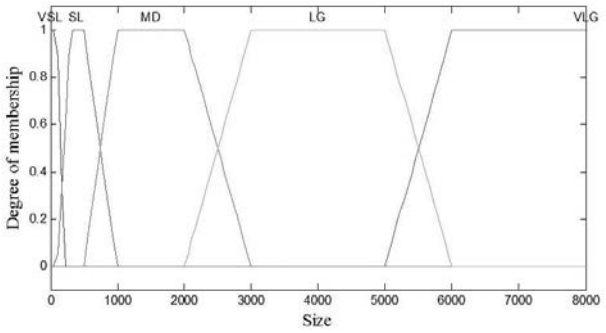

Fig. 21. Size fuzzy variable with five linguistic terms.

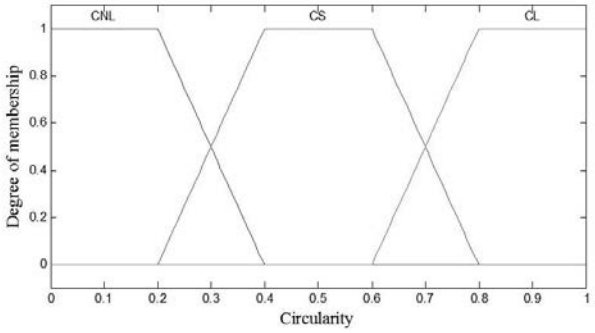

Fig. 22. Circularity fuzzy variable with three linguistic terms.

$$f_A(x) = \begin{cases} 0, & (x < a_A) \\ \dfrac{x - a_A}{b_A - a_A}, & (a_A \leq x < b_A) \\ 1, & (b_A \leq x < c_A) \\ \dfrac{d_A - x}{d_A - c_A}, & (c_A \leq x < d_A) \\ 0, & (x \geq d_A) \end{cases} \quad \ldots . \quad (8)$$

Figure 21 illustrates an example for a size fuzzy variable with five linguistic terms. The membership degree is usually a value in the range $[0,1]$, where 1 denotes a full membership and 0 denotes no membership.

For our cases, we define five fuzzy sets for the bright area size, including *verysmall* (*VSL*), *small* (*SL*), *medium* (*MD*), *large* (*LG*) and *verylarge* (*VLG*), as shown in **Fig. 21**, and define three fuzzy sets for the bright area circularity including *circle-no-like* (*CNL*), *circle-similar* (*CS*), *circle-like* (*CL*), as shown in **Fig. 22**. For the probability of cancer in an area, we define five sets for the output of fuzzy reasoning including *unlikely* (*UL*), *perhaps* (*PH*), *presumably* (*PM*), likely (*BL*), *surely* (*SR*).

We use $x = (s, e)$ to denote the input of our fuzzy inference mechanism, where s is bright area size, and e is bright area circularity, u is the output of our fuzzy inference mechanism and denote the probability of cancer. The fuzzy inference rules are denoted as follows:

Rule VSL-CNL: *IF (s is VSL) AND (e is CNL) THEN u is UL*

.....

Rule VLG-CL*: IF s is VLG) AND (e is CL) THEN u is BL*

Figure 23 shows the result of fuzzy inference on global temporal subtraction images in Case 2, where there is only one pathological change area, as marked in the original radiographs. We use gray level to denote the probability of cancer at each level, the higher of the gray level means the higher probability of cancer. To provide further selection, we also show the most cancer-like areas, for which the fuzzy inference outputs meet condition $u \geq BL$.

5. Conclusions

This paper has proposed a mutual-information-based global matching method for chest-radiography temporal subtraction. Experiment results have demonstrated that our proposed method enhances pathological changes, and reduces misregistration artifacts caused by patients posture and breathing. Although our proposed global matching method ensures the continuity of the subtraction image, there are still misregistration artifacts in some local areas. We also use local matching and fuzzy diagnosis on the experiment results. Our proposed method makes some improvement, but it is not very distinct. Moreover, we can see many mosaics in images after local matching. Improving local matching while keeping the continuity of a temporal subtraction image is thus an important issue for us to deal with in the future.

Acknowledgements

We thank the referees for their valuable comments which have greatly improved this paper. This work was supported in part by the Hori Science & Arts Foundation and the Ministry of Education, Science, Sports and Culture, Japan, Grant-in-Aid for Scientific Research (C), 23500222, 2011.

References:

[1] International Agency for Research on Cancer, "GLOBACAN," 2008. http://globocan.iarc.fr/

[2] T. Ishida, K. Ashizawa, R. M. Engelmann, S. Katsuragawa, H. MacMahon, and K. Doi, "Application of temporal subtraction for detection of interval changes in chest Radiographs: Improvement of subtraction image using automated initial image matching," J. of Dig. Imag., Vol.12, No.2, pp. 77-86, 1999.

[3] T. Ishida, S. Katsuragawa, K. Nakamura, H. MacMahon, and K. Doi, "Iterative image warping technique for temporal subtraction of sequential chest radiographs to detect interval change," Med. Phys., Vol.26, No.7, pp. 1320-1329, 1999.

[4] S. G. Armato III, D. J. Doshi, R. Engelmann, C. L. Croteau, and H. MacMahon, "Temporal subtraction in chest radiography: Automated assessment of registration accuracy," Med. Phys., Vol.33, No.5, pp. 1239-1249, 2006.

[5] T. Inaba, L. He, K. Suzuki, K. Murakami, and Y. Chao, "A Genetic-Algorithm-Based Temporal Subtraction for Chest Radiographs," J. of Advanced Computational Intelligence and Intelligent Informatics, Vol.13, No.3 pp. 289-296, 2009.

[6] B. Zitova and J. F1usser, "Image registration methods: A survey," Image and Vision Computing, Vol.21, No.11, pp. 977-1000, 2003.

[7] F. Maes, D. Vandermeulen, and P. Suetens, "Medical Image Registration Using Mutual Information," Proc. of The IEEE, Vol.91, No.10, pp. 1699-1722, 2003.

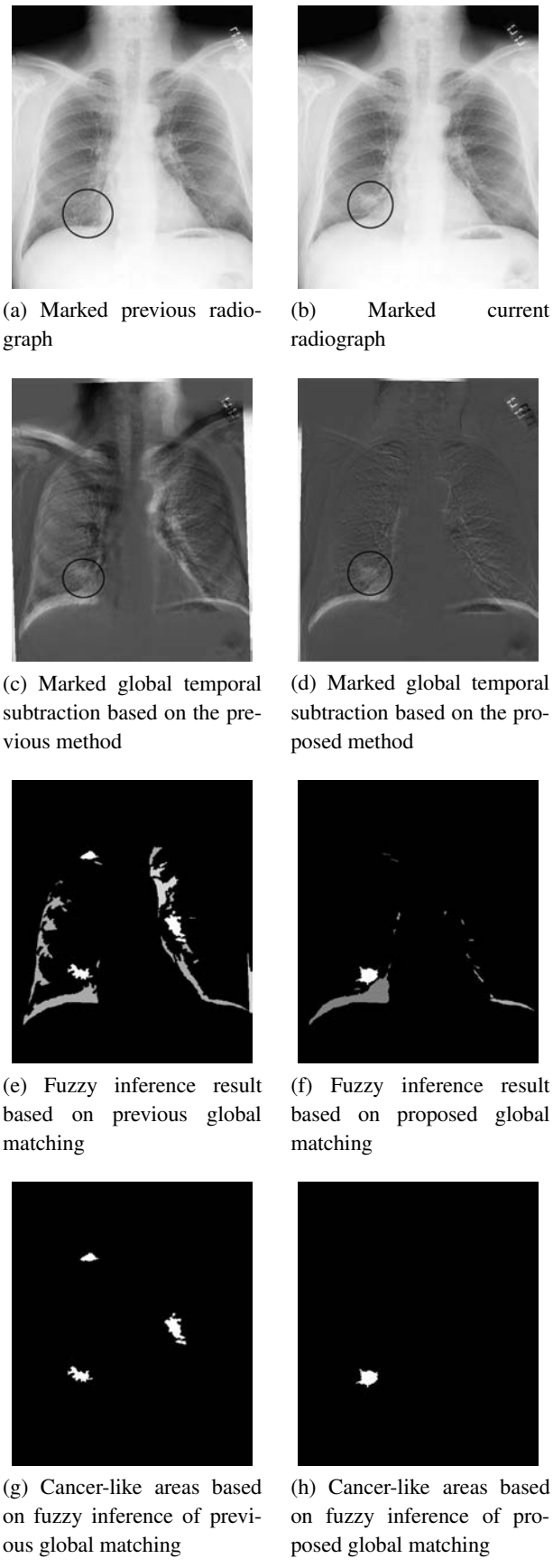

(a) Marked previous radiograph

(b) Marked current radiograph

(c) Marked global temporal subtraction based on the previous method

(d) Marked global temporal subtraction based on the proposed method

(e) Fuzzy inference result based on previous global matching

(f) Fuzzy inference result based on proposed global matching

(g) Cancer-like areas based on fuzzy inference of previous global matching

(h) Cancer-like areas based on fuzzy inference of proposed global matching

Fig. 23. Result of fuzzy inference on the global temporal subtraction images in Case 2.

[8] O. Folorunso, O. R. Vincent, and B. M. Dansu, "Image edge detection: A knowledge management technique for visual scene analysis," Information Management and Computer Security, Vol.15, No.1, pp. 23-32, 2007.
[9] J. F. Canny, "A Computational Approach to Edge Detection," IEEE Trans. Pattern Analysis and Machine Intelligence, Vol.8, No.6, pp. 679-698, 1986.
[10] L. He, Y. Chao, K. Suzuki, and K. Wu, "Fast Connected-Component Labeling," Pattern Recognition, Vol.42, pp. 1977-1987, 2009.

Name:
Qian Yu

Affiliation:
Department of Computer Science and Engineering, Nagoya Institute of Technology

Address:
Gokiso-cho, Showa-ku, Nagoya, Aichi 466-8555, Japan

Brief Biographical History:
2002-2006 B.E., Huazhong University of Science & Technology, China
2006-2009 M.E., East China Normal University, China
2010- D.E., Naogya Institute of Technology

Name:
Lifeng He

Affiliation:
Academic Dean, College of Electrical & Information Engineering, Shaanxi University of Science and Technology
Professor, Graduate School of Information Science and Technology, Aichi Prefectural University

Address:
Nagakute-cho, Aichi 480-1198, Japan

Brief Biographical History:
1997 Ph.D. degrees in AI and Computer Science from Nagoya Institute of Technology
1999- Associate Professor, Aichi Prefectural University
2006-2007 Research Associate, The University of Chicago, USA
2012- Professor, Aichi Prefectural University

Main Works:
• "Two Efficient Label-Equivalence-Based Connected-Component Labeling Algorithms for Three-Dimensional Binary Images," IEEE Trans. on Image Processing, Vol.20, No.8, pp. 2122-2134, 2011.
• "Fast Connected-Component Labeling," Pattern Recognition, Vol.42, pp. 1977-1987, 2009.
• "A Run-based Two-Scan Labeling Algorithm," IEEE Trans. on Image Processing, Vol.17, No.5, pp. 749-756, 2008.

Membership in Academic Societies:
• The Institute of Electrical and Electronics Engineers (IEEE), Senior Member
• Associate for Automated Reasoning (AAR)

Name:
Tsuyoshi Nakamura

Affiliation:
Associate Professor, Department of Computer Science and Engineering, Nagoya Institute of Technology

Address:
Gokiso-cho, Showa-ku, Nagoya, Aichi 466-8555, Japan

Brief Biographical History:
1998 Ph.D., Nagoya Institute of Technology
1998- Research Associate, Nagoya Institute of Technology
2003- Associate Professor, Nagoya Institute of Technology

Main Works:
• "Color transfer based on hierarchical image-region matching with interactive evolutionary computation," Kansei Engineering Int., Vol.5, No.4, pp. 1-10, 2006.

Membership in Academic Societies:
• The Institute of Electrical and Electronics Engineering (IEEE)
• Association for Computing Machinery (ACM)
• The Institute of Electronics, Information and Communication Engineers (IEICE)
• Japan Society for Fuzzy Theory and Intelligent Informatics (SOFT)
• Japan Society of Kansei Engineering (JSKE)

Name:
Yuyan Chao

Affiliation:
Professor, Graduate School of Environmental Management, Nagoya Sangyo University

Address:
Owariasahi-city, Aichi 488-8711, Japan

Brief Biographical History:
2000 Ph.D. degrees from Nagoya University
2000-2002 Special Foreign Researcher of Japan Society for the Promotion of Science, Nagoya Institute of Technology
2004- Associate Professor, Nagoya Sangyo University
2010- Professor, Nagoya Sangyo University

Main Works:
• "Two Efficient Label-Equivalence-Based Connected-Component Labeling Algorithms for Three-Dimensional Binary Images," IEEE Trans. on Image Processing, Vol.20, No.8, pp. 2122-2134, 2011.
• "Fast Connected-Component Labeling," Pattern Recognition, Vol.42, pp. 1977-1987, 2009.
• "A Run-based Two-Scan Labeling Algorithm," IEEE Trans. on Image Processing, Vol.17, No.5, pp. 749-756, 2008.

Membership in Academic Societies:
• Japanese Society for Artificial Intelligence (JSAI)

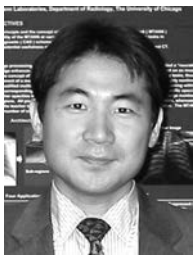

Name:
Kenji Suzuki

Affiliation:
Assistant Professor, Department of Radiology, Division of the Biological Sciences, The University of Chicago

Address:
P-104A, 5841 South Maryland Avenue, MC 2026 Chicago, IL 60637, USA

Brief Biographical History:
2001 Ph.D., Nagoya University
2001-2006 Research Associate, The University of Chicago, USA
2006- Assistant Professor, The University of Chicago, USA

Main Works:
• "Computer-aided detection of false-negative polyps in a multicenter clinical trial," Medical Physics, Vol.30, pp. 12-21, 2010.
• "Image-processing technique for suppressing ribs in chest radiographs by means of massive training artificial neural network (MTANN)," IEEE Trans. on Medical Imaging, Vol.25, pp. 406-416, 2006.
• "Separation of ribs and soft tissue in single chest radiographs by means of massive training artificial neural networks," Radiology, Vol.233, p. 291, 2004.

Membership in Academic Societies:
• Invited Associate Editor of Medical Physics
• Editor-in-Chief of International Journal of Intelligent Information Processing
• Editorial Board Member of Algorithms
• The Institute of Electrical and Electronics Engineers (IEEE), Senior Member